

# Enhancing current density profile control in tokamak experiments using iterative learning control

Federico Felici<sup>1</sup>, Tom Oomen<sup>1</sup> and the TCV team<sup>2</sup>

**Abstract**—Tokamaks are toroidal devices to create and confine high-temperature plasmas, and are presently at the forefront of nuclear fusion research. Many parameters in a tokamak are feedback controlled, but some quantities that are either difficult to measure or difficult to control are still controlled by trial-and-error adjustments of feedforward signals. For example, the current density profile plays an essential role in the confinement and stability properties of a tokamak plasma but only few demonstrations exist of feedback control, partly due to the unavailability of the measured variables in real-time on many tokamaks. The aim of this paper is to enhance the control of the current density profile by using batch-to-batch control. An iterative learning controller (ILC) is designed for the current density profile control problem. A simulation study for the future ITER tokamak is shown in which ILC is used to obtain a desired current density profile at the end of the plasma ramp-up phase. Experimental application of ILC to plasma discharges in the TCV tokamak is presented, where the time trajectory of the plasma internal inductance, a scalar measure of the current density profile width, is controlled by varying the total plasma current. Both demonstrate the feasibility of the proposed approach and encourage more extensive use of ILC in tokamak experiments.

## I. INTRODUCTION

Nuclear Fusion is the process whereby two light ions combine to form a heavier one, liberating energy. One promising method to achieve the high temperatures required for this process on earth is to confine a hot plasma using a device called a tokamak [1], which features an axisymmetric, toroidally shaped magnetic field configuration. Tokamaks are pulsed devices, in which the plasma is created, sustained, and then ramped down in a process known as a ‘shot’ or ‘discharge’. During each discharge, a number of feedback control loops are used to control key parameters of the discharge. For a general overview of tokamak plasma control, see [2] [3].

While feedback control of some parameters of a tokamak (e.g. position, shape, plasma current, stored energy) is routinely performed, control of many other quantities is less routine (e.g. current density profile, pressure profile, density profile, internal plasma inductance) and in many

cases parameters are still controlled by trial-and-error adjustment of feedforward signals. Several reasons can be indicated to explain this. Firstly, some quantities are essential for tokamak stability and had to be controlled since the early stages of tokamak research, while control of many other quantities is optional, improving the performance and reproducibility but often not strictly necessary for the physics studies which are the focus of many present-day experiments. Also, many controlled variables are not measured in real-time but have to be reconstructed a-posteriori by merging information from several measurements in complicated post-shot analysis procedures.

One important quantity that is not yet controlled in real-time routinely is the current density profile. This plays an important role in the stability and confinement performance of the plasma, thus defining whether the conditions for fusion can be achieved. Extensive research has recently been carried out on feedback control of the current density profile, in both simulations [4], [5], [6], [7], [8] and experiments [9], [10], [11], [12]. Feedback control is a very promising solution, but is unfortunately rarely applied in existing tokamaks. One reason is that on many tokamaks the current density profile can presently not be determined in real-time with sufficient accuracy for feedback control, mostly due to lack of reliable measurements. In other cases, tokamak operators appear reluctant to relinquish control over some key variables to feedback controllers since they may affect the experiment in an unexpected manner, and may lead to losing highly scarce experimental time.

Purely feedforward-based control methods have also been suggested and studies of actuator trajectory optimisation for current density profile control have been presented in [13], [14], [15]. While these are also promising as tools for preparing a plasma discharge, without some form of feedback the inevitable model mismatch will result in errors in the profiles obtained in actual experiments.

Although important steps have been taken on both feedforward and feedback control, they are at present rarely applied due to the mentioned disadvantages of each approach, resulting in poor open-loop control performance. This paper aims to develop a batch-to-batch control approach for the current density profile that combines advantages of feedforward and feedback control, and does not suffer from the above disadvantages.

The potential of batch-to-batch control techniques, where the error from a previous trial is used as feedback signal to design a feedforward input for the next trial, has remained relatively unexplored in the context of tokamak control. In

<sup>1</sup> Eindhoven University of Technology, Faculty of Mechanical Engineering, Control Systems Technology group, P.O. Box 513, 5600 MB Eindhoven, The Netherlands. f.felici@tue.nl

<sup>2</sup> École Polytechnique Fédérale de Lausanne (EPFL), center de Recherches en Physique des Plasmas, CH-1015 Lausanne, Switzerland.

This work is supported by the Innovational Research Incentives Scheme via the VENI grants: “Control of plasma profiles in a fusion reactor” (no. 680.47.436) and “Precision Motion: Beyond the Nanometer” (no. 13073) awarded by NWO (The Netherlands Organisation for Scientific Research) and STW (Dutch Science Foundation).

this paper, a batch-to-batch control technique is proposed for tokamak control problems, complementary to ongoing efforts on feedback and feedforward control, specifically to improve feedforward trajectories when feedback is not (yet) practical, possible, or desired. In addition, if feedback control is implemented, batch-to-batch control can still be used to improve the control performance since it does not suffer from causality constraints in the physical time domain [16].

Iterative Learning Control (ILC) is one such batch-to-batch control method that is specially suited for repetitive control problems. It has been applied to various applications including robot arms [17], wafer scanners [18] and printing systems [19]. In this paper, we present the application of ILC to the tokamak current density profile control problem for the first time in both simulation and experiment.

There are some interesting differences between the application of ILC to tokamak control problems in this paper with respect to mechatronic applications. While ILC in mechatronics systems is used to as add-on to feedback controlled systems to enhance the performance by designing a better feedforward input, ILC is used here as stand-alone method to iteratively design feedforward signals for a situation where feedback control is not used. Also, a key ingredient in ILC is a dynamical model of the system. ILC in mechatronics applications is commonly based on lumped-parameter systems that are well described by linear-time-invariant (LTI) models and can be readily simulated. Instead, the evolution of tokamak plasma profiles is described by a set of nonlinear PDEs. In this paper these PDEs are discretised to yield a set of nonlinear ODEs. These are solved, and a linear-time-varying (LTV) model is simultaneously determined around the nonlinear trajectory. This (locally valid) LTV model is used as input for the ILC method.

Indeed, tokamak current density profile control was mentioned previously in [20] as a motivation to study the application of ILC to distributed parameter systems described by linear, parabolic PDEs in infinite-dimensional setting and tested on a heat diffusion equation with constant coefficients. In the present work, a very different approach is taken and ILC is applied to a discretized, nonlinear model for tokamak plasma profile behaviour and tested in both simulation and experiment.

The rest of this paper is structured as follows. In Section II, we first present a rationale for the use of ILC in tokamak control in general, outlining some of the peculiarities of tokamak control that make ILC a particularly attractive option for a variety of control problems. Section III describes the physical PDE model describing tokamak current density profile diffusion and the controlled variables. In Section IV the ILC algorithm is formulated for our particular problem. Next, results of applying ILC to the current profile control problem in both simulation (Section V) and experiment (Section VI) are shown. Other tokamak control problems which may benefit from batch-to-batch control solutions, as well as the conclusions, are presented Section VII.

## II. APPLYING ILC TO TOKAMAK CONTROL

In this section we will present the main reasons why ILC appears particularly useful for tokamak plasma control. We begin by mentioning some characteristics of tokamak control problems and then point out which properties of ILC match well with these characteristics.

### A. Tokamak control characteristics and constraints

Tokamak control problems have some specific characteristics and constraints, listed below.

- T1 Tokamaks are repetitive systems. Since the confining plasma current usually has to be induced by external coils, limits on the current in these coils mean that the plasma can not be sustained indefinitely. This pulsed character means that the same, or very similar, plasmas are created multiple times. Even if the entire discharge is not the same, the crucial, initial part of the discharge in which the plasma is established, called the ramp-up, is often the same for many shots and is the result of careful fine-tuning.
- T2 Measurements of high-temperature plasmas are technologically difficult, therefore not all measurements are available in real-time for use in a feedback controller. Many plasma parameters become known only after dedicated post-shot analysis and interpretation of discharge data, which often required human intervention and validation. While significant effort is being put on integrating an increasing number of measurements into plasma real-time control systems, including ongoing work on model-based state observers for plasma current density profile [21], this is not always possible nor practical, particularly in the initial phase of a new tokamak's operational life when many sensor systems are simply not ready or not immediately integrated with the real-time control system.
- T3 Adoption of feedback controllers is often constrained in practice by the fear of many discharges being required for commissioning and tuning of each controller for a particular operating scenario. Therefore many quantities are feedforward-controlled.
- T4 Physical models of the processes are available in a suitable form. Though complete first-principles-based models for tokamak plasmas are difficult and time-consuming to simulate, a number of control-oriented models for the evolution of the variables of interest are available.
- T5 Amplitude and state constraints are ubiquitous in tokamaks. Actuator power and ramp rates are limited by technological constraints and systems are usually operated close to their maximum capacity. Constraints in the operating space, originating from plasma stability limits, translate into state constraints for the control problem. Some actuators, in particular gas valves, often have a time delay as well.

### B. Properties of Iterative Learning Control

Iterative Learning Control is a data-driven control methodology that aims to enhance performance by learning from

previous experiments [16], [22]. Data from the previous experiment, or *trial*, is used as feedback signal to design a feedforward trajectory for the next trial. It is particularly suited for repetitive control tasks, where the same reference has to be tracked for many consecutive trials. At each trial, the residual error is used together with a dynamic model of the system to design an improved feedforward trajectory for the next trial. As such, ILC is particularly suited for processes which:

- I1 Are repetitive, having to follow the same or similar reference trajectories each time.
- I2 Have controlled variables that are difficult or costly to measure in real-time for feedback control purposes.
- I3 Are presently controlled with a strong feedforward component and little or no feedback, for example because time delays limit the feedback performance.
- I4 Have a reasonably accurate (linearized) dynamic model describing the input-output behaviour of the process.
- I5 Have limits in both actuator and states, which can be included [23] in the ILC problem.

ILC characteristics I1-I5 are well-aligned with tokamak control issues and constraints T1-T5 mentioned above, motivating the use of ILC in tokamak control problems. In the remainder of this paper we will present the application of ILC to the special case of current profile diffusion. Other examples will be discussed in Section VII.

### III. MODEL AND SIMULATION OF TOKAMAK PLASMA CURRENT DIFFUSION

In this section we present a dynamical model of tokamak plasma current diffusion and introduce the two variables which will be controlled in the examples shown in the later sections. This model will also be the basis for deriving a linearized model for the system that will be used for ILC, as we shall see in Section IV.

#### A. Model for tokamak profile dynamics

Due to the (spatially varying) resistivity of the plasma, the electrical current will naturally distribute itself in such a way that the electric field becomes constant inside the plasma. This occurs on the so-called resistive time scale which ranges from hundreds of milliseconds for present-day tokamaks such as TCV to hundreds of seconds for large tokamaks such as ITER. To model the plasma evolution more accurately, this equation is solved together with an equation for the energy transport. This evolves on a faster timescale than the flux diffusion and is nonlinearly coupled to the latter.

The two coupled equations can be written as:

$$k_1 \frac{\partial \psi}{\partial t} = \frac{\partial}{\partial \rho} k_2 \frac{\partial \psi}{\partial \rho} + k_3 + \sum_{i=1}^{n_u-1} k_{u,i} u_i \quad (1)$$

$$c_1 \frac{\partial T_e}{\partial t} = \frac{\partial}{\partial \rho} c_2 \frac{\partial T_e}{\partial \rho} + c_3 + \sum_{i=1}^{n_u-1} c_{u,i} u_i \quad (2)$$

This represents two diffusion equations for the distributed variables  $\psi$  and  $T_e$ , which are, respectively, the poloidal magnetic flux, and electron temperature as a function of

the 1D radial coordinate  $\rho = \rho_{tor}$ . This radial coordinate is related to the square root of the toroidal magnetic flux enclosed by surface of constant poloidal flux (see e.g. [24] for a more detailed treatment),  $\rho = 0$  corresponds to the plasma core and  $\rho = 1$  at the value at the plasma edge. The quantities  $k_1, k_2, k_3, c_1, c_2, c_3$  are functions of  $\rho$ , which are nonlinearly dependent on the variables  $\psi$  and  $T_e$ .

The externally driven current density and applied heating (e.g. by plasma auxiliary heating systems) are modeled using  $k_{u,i}$  and  $c_{u,i}$ , which are also a function of  $\rho, T_e$  and  $\psi$ , that determine the spatial localization of each of the  $n_u - 1$  auxiliary actuators. The input  $u_i = P_{aux,i} \in \mathbb{R}$  corresponds to the power of the  $i$ th heating and current drive actuator. As a boundary condition for (1), the total plasma current  $I_p$  is prescribed at the outer edge of the plasma as  $\left. \frac{\partial \psi}{\partial \rho} \right|_{\rho=1} = k_{I_p} I_p$  where  $k_{I_p}$  is a known scalar. Therefore  $I_p(t)$  can be viewed as an additional input to the equation and can be used to control the time-behaviour of  $\psi(\rho, t)$ , and the system can be recognized as having  $n_u$  inputs in total. A Dirichlet boundary condition is prescribed for (2) as  $T_e|_{\rho=1} = T_{e,1}$ .

Models of this type have been used in the past for designing and testing feedback controllers (e.g. [10], [8]) and observers [21] for the current density profile.

#### B. Controlled variables

The controlled variables of interest for the present study are the  $q$  profile and the internal inductance  $\ell_i$ . The  $q$  profile is a function of  $\rho$ , defined as:

$$q(\rho) = 1/\iota(\rho), \text{ where } \iota = \frac{1}{2\Phi_b} \frac{\partial \psi}{\partial \rho} \quad (3)$$

and  $\Phi_b \in \mathbb{R}$  is a known scalar representing the total toroidal flux enclosed by the last closed flux surface. Note that while  $q$  is a nonlinear function of  $\frac{\partial \psi}{\partial \rho}$ , its inverse  $\iota$  is linear in  $\frac{\partial \psi}{\partial \rho}$ , so  $\iota$  will be controlled instead of  $q$ , for convenience.

The internal inductance  $\ell_i \in \mathbb{R}$  is defined as

$$\ell_i(t) = \int_0^{\rho_b} c_\ell \left( \frac{\partial \psi}{\partial \rho} \right)^2 d\rho \quad (4)$$

Where  $c_\ell(\rho)$  is a known function. Clearly  $\ell_i$  is a nonlinear function of  $\psi(\rho, t)$ .

#### C. Numerical solution

Since the system of equations (1)-(2) is numerically stiff, specialized simulation codes are necessary to solve the coupled system. One such code, that we will use in this paper, is RAPTOR [14], a code developed purposely for real-time control applications. One of its main advantages is that it returns not only the solution (in time) of the nonlinear PDEs, but also the local linearization around the nonlinear trajectory. In this code, (1)-(2) are discretized in space using finite elements and in time using a backwards Euler scheme, yielding a set of implicit discrete-time ODEs which are solved using a Newton method.

#### IV. ILC PROBLEM FORMULATION FOR LTV SYSTEMS AROUND A NOMINAL TRAJECTORY

We formulate the ILC problem in discrete-time as determining the variation  $\Delta u$  in the feedforward input to be applied at the next trial, that minimizes a cost function  $J \in \mathbb{R}$ , subject to constraints:

$$\Delta u = \arg \min_{\Delta u} J, \quad \text{subject to} \quad A\Delta u \leq b \quad (5)$$

Each term will be discussed in the remainder of this section. We shall first construct an expression for  $J$  involving the expected error on the next trial as a function of the change of input at the next trial.

##### A. Linearized expression for the error on the next trial

A linearized time-varying (LTV) model is constructed around a nominal solution of the nonlinear system (1)-(2) with output equation (3) or (4). Details of the linearization procedure and its validation can be found in [8].

Let  $u_k^o \in \mathbb{R}^{n_u} \forall k \in [1, \dots, N]$  be a (time-discretized) input vector sequence for the spatially discretized model derived from the PDE model, and let  $x_k^o$  and  $y_k^o$  be corresponding state and output vectors. We can then derive an LTV model for the system around this nominal trajectory by defining  $u_k = u_k^o + \delta u_k$ ,  $x_k = x_k^o + \delta x_k$  and  $y_k = y_k^o + \delta y_k$ , and writing:

$$\delta x_{k+1} = A_k \delta x_k + B_k \delta u_k \quad (6)$$

$$\delta y_k = C_k \delta x_k + D_k \delta u_k \quad (7)$$

Now, let the vectors for each  $k$  be stacked into a single vector as  $\bar{y}^T = [y_1^T, y_2^T, \dots, y_N^T]^T \in \mathbb{R}^{Nn_y}$ , and analogously for  $\bar{u}$ ,  $\delta \bar{y}$ ,  $\delta \bar{u}$ ,  $\delta \bar{y}^o$  and  $\delta \bar{u}^o$ . Then one can easily show that

$$\delta \bar{y} = \mathcal{T} \delta \bar{u} + \mathcal{D} d \quad (8)$$

in which  $\mathcal{T} \in \mathbb{R}^{Nn_y \times Nn_u}$  is a matrix with only the lower triangular elements populated,  $\mathcal{D} \in \mathbb{R}^{Nn_y \times n_a}$  is a matrix describing the effect of a disturbance vector  $d \in \mathbb{R}^{n_a}$ , that is modeled as a constant, on the output. We also assume a constant initial condition  $\delta x_0$  that is included in  $d$  for simplicity.  $\mathcal{T}$  and  $\mathcal{D}$  can be constructed from the system matrices  $A_k$ ,  $B_k$ ,  $C_k$ ,  $D_k$  and from knowledge of the disturbance model. Defining the references for  $\bar{y}$  as  $\bar{r}$ , let the error vector for the  $j$ th trial be

$$\bar{e}^j = \bar{r} - \bar{y}^j. \quad (9)$$

Using  $\bar{y}^j = \bar{y}^{j,o} + \delta \bar{y}^j$  and (8) one can write

$$\bar{e}^j = \bar{r} - (\mathcal{T} \delta \bar{u}^j + \mathcal{D} d) - \bar{y}^{j,o} \quad (10)$$

from which we can write the expected error at the next trial as a function of  $\bar{u}^{j+1}$ :

$$\bar{e}^{j+1} = \bar{r} - (\mathcal{T} \delta \bar{u}^{j+1} + \mathcal{D} d) - \bar{y}^{j,o} \quad (11)$$

Substituting  $\bar{r}$  from (10), we see that

$$\bar{e}^{j+1} = \bar{e}^j - \mathcal{T}(\delta \bar{u}^{j+1} - \delta \bar{u}^j) \quad (12)$$

and the effect of the constant disturbances and the nominal output trajectory cancel. Since  $\bar{u}^j$  and  $\bar{e}^j$  are known after

the  $j$ th trial, (12) effectively gives the relation between the error expected at the next trial  $\bar{e}^{j+1}$  and the next input trajectory perturbation  $\delta \bar{u}^{j+1}$ . Naturally the equality holds only if the perturbation dynamics is exactly described by the LTV model, otherwise the equality will be only approximate. Note also that one has the choice whether to update the LTV model based  $\bar{u}^{j,o} = \bar{u}^j$ , which will likely be more accurate, or to keep the nominal LTV model determined with the original feedforward signal  $u^{j,o} = \bar{u}^0 \forall j$ .

##### B. Cost function and constraints

The ILC algorithm is formulated as aiming, at each trial, to compute the (total) feedforward trajectory for the next trial:  $\bar{u}^{j,o} + \delta \bar{u}^{j+1}$  that minimizes a weighted norm of  $\bar{e}^{j+1}$ , plus some regularizing terms that depend on  $\delta \bar{u}^{j+1}$ . This is all written in the cost function:

$$J = \|W_e \bar{e}^{j+1}\|_2^2 + \|W_u (\bar{u}^{j,o} + \delta \bar{u}^{j+1} - \bar{u}^0)\|_2^2 + \|W_{\Delta u} (\delta \bar{u}^{j+1} - \delta \bar{u}^j)\|_2^2 \quad (13)$$

Each term will be discussed in detail below:

- P1 Penalty on (linear combinations of) the error at the next iteration. A typical choice is  $W_e = w_e I_{Nn_y}$  where  $I_{Nn_y}$  is the  $(Nn_y) \times (Nn_y)$  identity matrix.
- P2 Penalty on the feedforward correction, attempting to maintain the feedforward input close to the original trajectory  $\bar{u}^0$  or penalizing its time derivative.  $W_u$  is typically structured as  $w_u I_{Nn_u} + w_{du} D$  where  $w_u \in \mathbb{R}$  and  $w_{du} \in \mathbb{R}$  are scalar weights and the matrix  $D$  is structured such that  $D \bar{u} \approx \frac{\partial \bar{u}}{\partial t}$ , typically by a finite difference approximation.
- P3 Penalty on the variation from one iteration to the next. This is particularly important for the problem studied here where an LTV model is constructed around a nonlinear trajectory, as taking too large steps could bring the system away from the region of validity of the linearised model (12). An adequate choice of this term is important to improve the convergence speed of the procedure, to achieve robustness against trial-varying disturbances and noise, and to reduce the required trials to achieve a given performance.

Substituting (12) and rewriting the equation in terms of  $\Delta \bar{u}^j = (\delta \bar{u}^{j+1} - \delta \bar{u}^j)$  and  $\bar{u}^{j0} = \bar{u}^j - \bar{u}^0$  yields

$$J = \|W_e (\bar{e}^j - \mathcal{T} \Delta \bar{u}^j)\|_2^2 + \|W_u (\bar{u}^{j0} + \Delta \bar{u}^j)\|_2^2 + \|W_{\Delta u} (\Delta \bar{u}^j)\|_2^2 \quad (14)$$

The cost function can be rewritten as a quadratic function of  $\Delta u$ :

$$J = \Delta \bar{u}^{j\top} H \Delta \bar{u}^j + f^\top \Delta \bar{u}^j + c \quad (15)$$

Where from (14) we can identify:

$$H = \mathcal{T}^\top W_e^\top W_e \mathcal{T} + W_u^\top W_u + W_{\Delta u}^\top W_{\Delta u} \quad (16)$$

$$f = -2\bar{e}^{j\top} (W_e^\top W_e \mathcal{T}_k) + 2\bar{u}^{j0\top} \mathcal{T} (W_u^\top W_u + W_g^\top W_g) \quad (17)$$

$$c = \bar{e}^{j\top} W_e^\top W_e \bar{e}^j + \bar{u}^{j0\top} (W_u^\top W_u + W_g^\top W_g) \bar{u}^{j0} \quad (18)$$

Constraints on the input trajectories, including limits on absolute values or ramp rates may be expressed as  $A^j \Delta \bar{u}^j \leq b^j$ , where any nonlinear constraints have to be linearised around the  $j$ th trajectory first.

If there are no inequality constraints, then an analytical solution to the problem (5) exists. In case of inequality constraints, this minimization problem can still be solved rapidly and efficiently using well-established numerical algorithms for QP problems [25], and global convergence is always guaranteed if  $H$  is positive definite. In practice, choosing the weighting matrices in the two last terms in (16) as positive diagonal matrices ensures positive definiteness of  $H$ , so this can always be satisfied. Solving (5) numerically for the system explored here the number of to-be-optimized control input parameter is of order  $\sim 100$ , takes no more than a few seconds on a modern CPU.

## V. APPLICATION OF ILC TO $q$ PROFILE CONTROL SIMULATIONS FOR THE ITER TOKAMAK

For tokamak discharges it can be important to establish a desired  $q$  profile at the end of the ramp-up of the plasma. Here we will show simulations of  $q$  profile control using ILC for the ITER tokamak, demonstrating that ILC is able to recover a nominal  $q$  following perturbation of the nominal model used to determine the desired, reference  $q$  profile.

### A. ILC cost function and constraint definition

The ILC problem is formulated in terms of the inverse of the safety factor profile,  $\iota = 1/q$ . This quantity is discretized on a radial grid of 31 points. The error is defined as

$$e_k = \iota_{ref} - \iota_k \quad (19)$$

where  $\iota_k \in \mathbb{R}^{31}$  is the  $\iota (= 1/q)$  profile sampled at the 31 radial locations and  $\iota_{ref}$  is a reference  $q$  profile.

For this demonstration, we aim to achieve small  $e_k$  at the end of the plasma current ramp-up phase at  $t = 140$ s. The ILC cost function is written as (13), where the error weight matrix  $W_e$  is chosen such that only the error at  $t = 140$ s is weighed. The other cost function weight matrices are constructed as follows:  $W_{\Delta u} = w_{\Delta u} I$  with  $w_{\Delta u} = 1.0 \times 10^{-8}$ ,  $W_u = w_{du} D$  with  $w_{du} = 1 \times 10^{-7}$  and  $D$  defined as in Section IV-B. We hence impose a penalty on the change of feedforward signal on each iteration, as well as the time derivative of the resulting total feedforward signal. The small values of the weights are caused by the scaling of the input parameters (typically of order  $10^6$ ) with respect to the outputs (typically order 1).

Given 4 actuator inputs and 31 controlled variables, we are dealing with a MIMO system with more outputs than inputs. For this reason alone it will therefore not be possible to control the error exactly to zero (even if the input weights are set to zero), but only to some nonzero (global) minimum.

The constraints are defined for the maximum and minimum plasma current and total auxiliary power values:

$$3.5\text{MA} \leq I_p \leq 13\text{MA} \quad (20)$$

$$0\text{MW} \leq \sum_i P_{aux,i} \leq 37\text{MW} \quad (21)$$

Additionally, the start and end values of the actuators are also kept fixed. Other constraints on e.g. actuator ramp-rates could trivially be added, but are not considered here.

### B. Procedure and simulation results

First, a feedforward-controlled simulation of the ITER plasma profile evolution during plasma ramp-up is carried out by solving equations (1)-(2). The inputs to the simulation are the time trajectory of the plasma current  $I_p(t) \in \mathbb{R}$  and of  $P_{aux,i} \in \mathbb{R}$ ,  $i \in [1, \dots, 3]$  the power to three sources of auxiliary heating and current drive, corresponding to  $u_i$  in (1)-(2). The simulation parameters used in this study are described in detail in [15]. For the present purposes, this simulation amounts to an optimized ramp-up simulation in which a nominal desired  $q$  profile is obtained.

When the obtained actuator trajectories are used in the true tokamak, the result will not exactly match the simulation due to inevitable model mismatches. In our case, we simulate the model mismatch by varying the coefficients of the thermal transport, resistivity and current drive efficiency in the simulation model. As can be observed in Figure 1, this yields a different  $q$  profile at the end of the ramp-up (bottom left, red), at  $t = 140$ s, than the nominal simulation (black). This is also due to the lower  $T_e$  profile, as is visible in Figure 1 (bottom-right, black vs red curve).

We then apply ILC control to recover the desired nominal  $q$  profile, iteratively adjusting the time trajectories of  $I_p$ , and  $P_{EC,i}$ . The LTV model that is used in the ILC algorithm is updated at each trial using the previous input trajectory. The resulting trajectories after 5 iterations are also shown in Figure 1 (blue). The bottom-left panel shows that the  $q$  profile indeed converges close to the nominal reference. The actuator time traces (top panels) show that this is achieved by changing the  $I_p$  trajectory and also by adjusting the power in each of the EC sources. The control focuses on achieving the correct  $q$  profile and does not change the temperature of the plasma, as this is not included as a controlled variable. This is shown in the bottom-right panel.

Figure 2 shows the evolution of the error over each trial. The profile error of  $\iota - \iota_{ref}$  is shown (left) as well the error norm  $J_e = \|W_e \bar{e}^j\|_2^2$  (right) for each iteration. This shows good convergence after already three iterations, with minor improvements in iterations 4 and 5. Clearly, it is not possible to obtain a truly zero error because there are more controlled variables than actuators and because the derivative of the trajectory is also penalized.

## VI. EXPERIMENTAL APPLICATION OF ILC TO INTERNAL INDUCTANCE CONTROL IN THE TCV TOKAMAK

### A. Problem formulation

This section describes an experimental demonstration of control of the internal inductance ( $\ell_i$ ) by varying the total plasma current  $I_p$  in the TCV tokamak [26]. The internal inductance is a single-parameter measure of the distribution of electrical current inside the tokamak as defined in (4). High  $\ell_i$  corresponds to a current density distribution peaked in the center of the plasma, and too high  $\ell_i$  can have

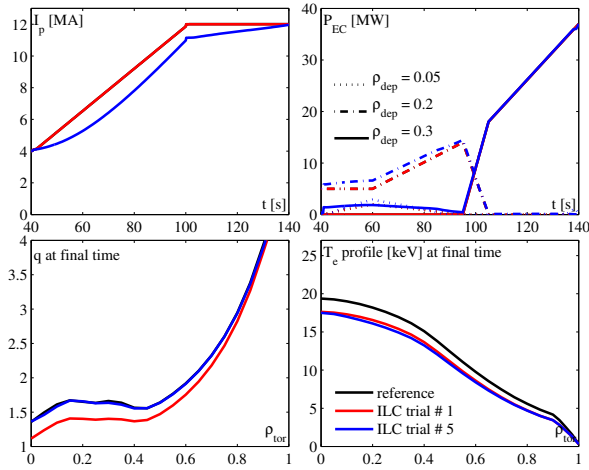


Fig. 1. ILC achieves an almost perfect final  $q$  profile in a simulated ITER advanced scenario plasma after 5 trials (bottom-left). Original (red) and modified (blue)  $I_p$  trajectory (top-left) and EC power trajectory for various radial position locations (top-right). Bottom panels:  $q$  profile (left) and  $T_e$  profile for the reference simulation (black), the first ILC trial (red) and the fifth ILC trial (blue). Note that the achieved  $q$  profile covers the reference, while the temperature ( $T_e$ ) profile remains different from the reference, as this variable is not controlled.

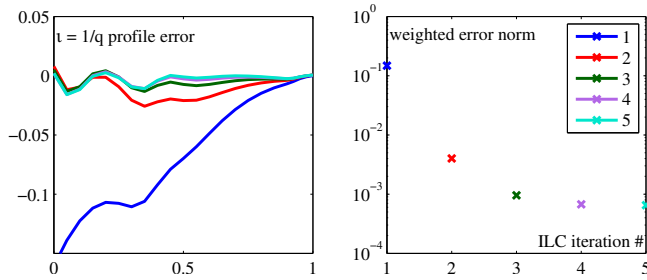


Fig. 2. Residual error of the  $\iota = 1/q$  profile with subsequent ILC iterations. Left panel: error of  $1/q$  for each ILC iteration. Right panel: error norm  $J_e = \|W_e \bar{e}^j\|_2^2$  per iteration.

detrimental effects on the plasma vertical position stability [27]. Low  $\ell_i$  corresponds to a broad current distribution, and if  $\ell_i$  is too low, internal magneto-hydrodynamic instabilities are more likely to occur [1].

The internal inductance can be controlled in several ways, one of which is via the time evolution of  $I_p$ , which is itself feedback controlled by time-varying currents in external magnetic coils. We will show that using ILC we can obtain a desired  $\ell_i$  trajectory in a few (5) trials.

### B. Choice of weights and constraints and ILC procedure

The chosen weights are shown in Figure 3. As can be seen, the weights are constructed so as to penalise deviations of the current in the initial phases of the experiment with respect to the initial trajectory, and the change for each successive trial.

No constraints were imposed for these experiments, instead the proposed  $I_p$  trajectory was manually inspected at each trial, and was found to always remain within operational limits without the need for explicit constraints.

The experimental procedure is outlined below:

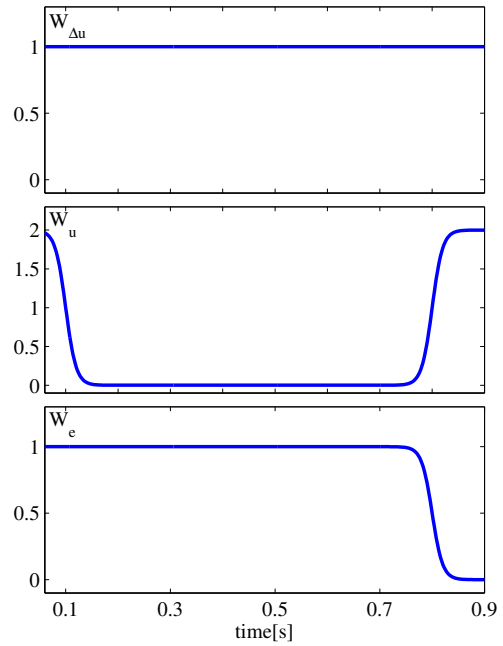


Fig. 3. Weight functions used in TCV experiments for  $\ell_i$  control. The error is weighed less in the regions close to the end of the region of interest, while actuator variations are penalized more, to discourage sudden steps in the input at the beginning of the ILC-controlled phase. A constant weight is applied to the variation of  $I_p$  between trials.

- 1) First, a plasma discharge was executed with a pre-programmed evolution of  $I_p$ , shown in blue in (Figure 4, top panel, blue). The resulting  $\ell_i$  trajectory was evaluated by processing measurements in the standard post-shot plasma state reconstruction algorithms, in particular the LIUQE equilibrium reconstruction code [28].
- 2) Then, a new reference  $\ell_i$  trajectory was chosen (Fig. 4, second panel, black line)
- 3) We then construct the LTV model describing the response of  $\ell_i(t)$  to changes in the input  $I_p(t)$ . This is done by first simulating the discharge by solving equations (1)-(2) with input  $I_p(t)$  using the RAPTOR code and then constructing the LTV model around the RAPTOR trajectory from the Jacobians as described in [8]. Note that no auxiliary heating power was used in these experiments, so, in (1),  $u = 0$  and the actuation comes purely from the boundary condition  $I_p(t)$ .
- 4) The ILC algorithm was run using the linearized model from step (3) and using the error between the reference and the obtained  $\ell_i$  as input. Solving the optimization problem yields an improved  $I_p$  trajectory for the next trial.
- 5) This new  $I_p$  reference trajectory was used as input for a new plasma discharge in TCV, which yields a new  $\ell_i$  trajectory.
- 6) Return to step 3.

Steps 3–6 were repeated a total of four times giving five trials in total including the original run.

### C. Results

The experimental time traces for each trial of the ILC control are shown in Figure 4. The top panel shows the

actuator trajectory  $I_p(t)$ , the second panel is the controlled output  $l_i(t)$ . Note how ILC generates a progressively different  $I_p$  trajectory and how the  $l_i$  trajectories are seen to converge close to the (black) reference trajectory. The lower three panels in Fig. 4 show the error, squared error, and time integrated square error, respectively. Clearly, the error decreases significantly between the first to the last iteration.

The evolution of the weighted error, per trial, is shown in Figure 5. As can be observed, the control error decreases on all trials but one. This might be due to model inaccuracies or trial-varying disturbances, and in any case does not necessarily entail that  $J$  itself is non-monotonic. Some error remains in the last phases of the experiment, but continuing this ILC procedure for further trials would most likely have reduced this error as well.

## VII. OUTLOOK

To conclude this paper, we mention three other tokamak control problems which may benefit from use of ILC.

- Plasma breakdown control – tokamak plasmas are initiated by generating a combined electric and magnetic field configuration that causes breakdown (ionization) of the gas in the vacuum chamber. The required currents in the surrounding coils can be pre-calculated, but uncertainties exist in the model. ILC can be used to iteratively improve the breakdown conditions by yielding a more suitable magnetic configuration at the desired breakdown time.
- Particle density control – this crucial parameter of a plasma discharge is regularly controlled in feedback in some devices, but often still in feedforward for many types of plasmas due to lack of reliable feedback controllers that work in all operating regimes. In some cases, time delays and nonlinearities in the gas valve actuators also cause problems in applying feedback control. Therefore, the density is often seen to evolve slightly during the discharge in response to disturbances and is often a primary reason why discharges have to be repeated.
- Radiation and heat flux control – The amount of radiated power can be controlled by injecting heavier elements (‘impurities’) into the plasma. This, and other factors like the magnetic field configuration play a role in the eventual heat flux reaching solid surfaces near the plasma. This is a relatively new topic of study, where some feedback control solutions have started to appear [29] but few are routinely used. Also here, lack of good real-time measurements of the controlled variables often limits the development of feedback control, and ILC could play a role in establishing appropriate feedforward signals iteratively.

We also see great potential in using rational basis function ILC [30] where ILC techniques are used to iteratively construct a feedforward controller that can handle trial-varying reference signals as well.

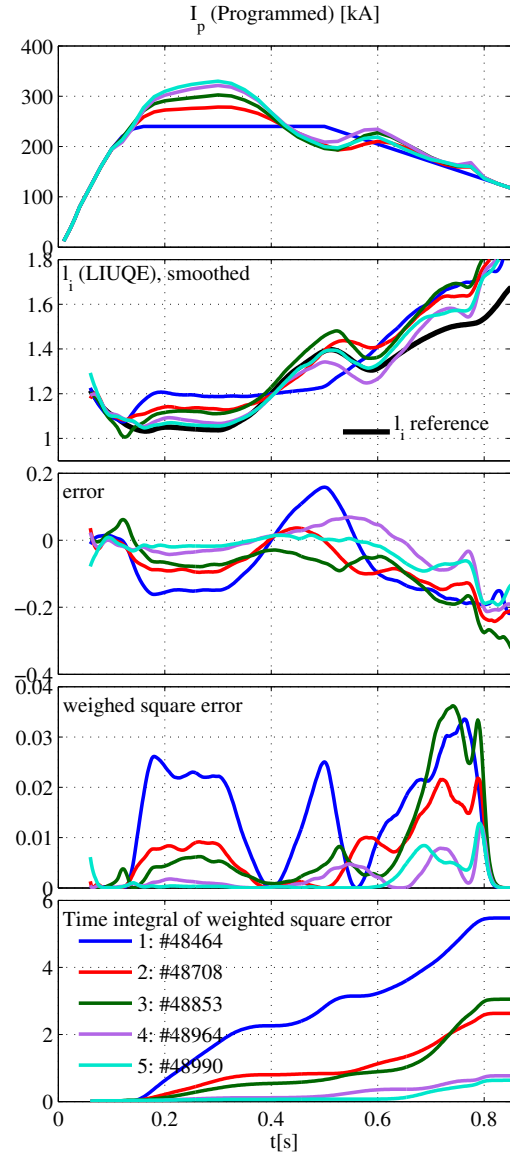


Fig. 4. Sequence of TCV shots converging to reference  $l_i$  trajectory. Sequence of  $I_p$  trajectories (first panel) and corresponding  $l_i$  trajectories compared to reference (black) (second panel). Weighted error in time (third panel), square error (fourth panel) and time-integral of weighted square error (fifth panel) show that the error decreases with each successive trial. The 5th trial (cyan) almost entirely overlaps the reference until  $t = 0.6$ s. Further improvement might be possible with further trials.

## VIII. CONCLUSIONS

This paper has explored the use of a batch-to-batch control technique for tokamak plasma current density profile for the first time. Successful results from both simulations and experiments applying Iterative Learning Control were shown.

End-point control of a distributed quantity closely related to the current density profile, the safety factor profile ( $q$ ), is demonstrated for simulations of ITER. It is shown that, also within 5 discharges, the  $q$  profile at the end of the simulation converges to values close to nominal reference profile. Control of the time-trajectory of a scalar parameter of the current density profile, the internal inductance, was demonstrated in experiments on the TCV tokamak. It was

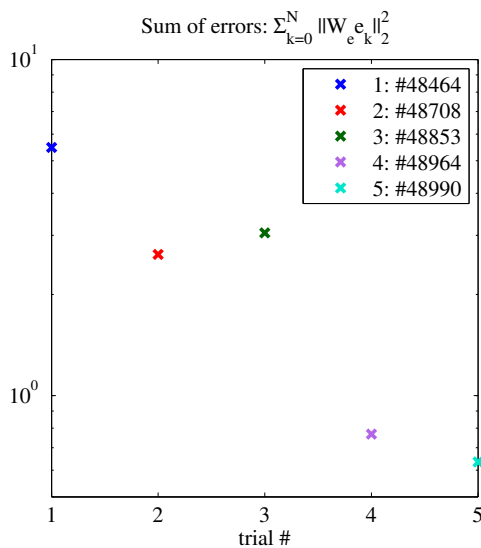


Fig. 5. Square error  $\sum_k \|W_{e_k}\|_2^2$  for successive trials, labeled according to the TCV shot number. Non-monotonic decrease of the error may be caused by the nonlinear nature of the system or by trial-varying disturbances, but the overall procedure is seen to converge.

shown that a reference trajectory for the internal inductance can be accurately tracked within 5 iterations by varying the time-evolution of the total plasma current. Both cases used LTV models linearised around the trajectory of the nonlinear model to construct cost function to be solved for each trial.

This work represents an interesting new and challenging application of ILC beyond its usual application to LTI systems, involving complex PDE-based models and linearisation around a nonlinear trajectory.

Based on the simulation and experimental results, it also seems that ILC is a promising tool for future tokamak experiments, for a variety of control problems other than current density profile control. It will help to minimize the degree of trial-and-error and bridging the gap between feedforward and feedback control in existing and future devices, cutting costs and saving valuable experiment time.

#### ACKNOWLEDGEMENT

F. Felici would like to thank Dr. S. Coda and Dr. O. Sauter for fruitful discussions and support in performing the TCV experiments described in Section VI.

#### REFERENCES

- [1] J. Wesson, *Tokamaks*, third edition ed., ser. International series of monographs on physics. New York (USA): Oxford Science Publications, 2004, vol. 118.
- [2] A. Pironti and M. Walker, "Control of tokamak plasmas: introduction to a special section," *Control Systems, IEEE*, vol. 25, no. 5, pp. 24 – 29, oct. 2005.
- [3] —, "Control of tokamak plasmas. ii," *Control Systems, IEEE*, vol. 26, no. 2, pp. 30 – 31, april 2006.
- [4] T. Tala, *et al.*, "Predictive transport simulations of real-time profile control in jet advanced tokamak plasmas," *Nuclear Fusion*, vol. 45, no. 9, p. 1027, 2005.
- [5] Y. Ou, *et al.*, "Optimal tracking control of current profile in tokamaks," *Control Systems Technology, IEEE Transactions on*, vol. 19, no. 2, pp. 432 –441, march 2011.
- [6] F. B. Argomedo, *et al.*, "Lyapunov-based distributed control of the safety-factor profile in a tokamak plasma," *Nuclear Fusion*, vol. 53, no. 3, p. 033005, 2013.

- [7] N. T. Vu, *et al.*, "IDA-PBC control for the coupled plasma poloidal magnetic flux and heat radial diffusion equations in tokamaks," in *Proceeding of the IFAC Congress, Cape Town, South Africa*, 2014.
- [8] E. Maljaars, *et al.*, "Control of the tokamak safety factor profile with time-varying constraints using mpc," *Nuclear Fusion*, vol. 55, no. 2, p. 023001, 2015.
- [9] D. Moreau, *et al.*, "A two-time-scale dynamic-model approach for magnetic and kinetic profile control in advanced tokamak scenarios on jet," *Nuclear Fusion*, vol. 48, no. 10, p. 106001, 2008.
- [10] J. E. Barton, *et al.*, "Toroidal current profile control during low confinement mode plasma discharges in DIII-D via first-principles-driven model-based robust control synthesis," *Nuclear Fusion*, vol. 52, no. 12, p. 123018, 2012.
- [11] J. A. Romero, *et al.*, "Current profile control using the ohmic heating coil in TCV," in *IAEA Conference 2012, San Diego, CA (USA)*, October 2012, pp. EX/P4–35.
- [12] M. Boyer, *et al.*, "Backstepping control of the toroidal plasma current profile in the DIII-D tokamak," *Control Systems Technology, IEEE Transactions on*, vol. 22, no. 5, pp. 1725–1739, Sept 2014.
- [13] C. Xu, *et al.*, "Ramp-up-phase current-profile control of tokamak plasmas via nonlinear programming," *Plasma Science, IEEE Transactions on*, vol. 38, no. 2, pp. 163 –173, February 2010.
- [14] F. Felici and O. Sauter, "Non-linear model-based optimization of actuator trajectories for tokamak plasma profile control," *Plasma Physics and Controlled Fusion*, vol. 54, no. 2, p. 025002, 2012.
- [15] J. van Dongen, *et al.*, "Numerical optimization of actuator trajectories for iter hybrid scenario profile evolution," *Plasma Physics and Controlled Fusion*, vol. 56, no. 12, p. 125008, 2014.
- [16] D. Bristow, M. Tharayil, and A. Alleyne, "A survey of iterative learning control," *Control Systems, IEEE*, vol. 26, no. 3, pp. 96–114, June 2006.
- [17] W. Messner, *et al.*, "A new adaptive learning rule," *IEEE Transactions on Automatic Control*, vol. 36, no. 2, pp. 188–197, February 1991.
- [18] S. Mishra, J. Coaplen, and M. Tomizuka, "Precision positioning of wafer scanners: Segmented iterative learning control for nonrepetitive disturbances [applications of control]," *IEEE Control Systems Magazine*, vol. 27, no. 4, pp. 20–25, 2007, cited By 40.
- [19] J. Bolder, *et al.*, "Using iterative learning control with basis functions to compensate medium deformation in a wide-format inkjet printer," *Mechatronics*, vol. 24, no. 8, pp. 944 – 953, 2014.
- [20] C. Xu, R. Arastoo, and E. Schuster, "On iterative learning control of parabolic distributed parameter systems," in *the 17th Mediterranean Conference on Control & Automation, Thessaloniki, Greece*, 2009.
- [21] F. Felici, M. de Baar, and M. Steinbuch, "A dynamic state observer for real-time reconstruction of the tokamak plasma profile state and disturbances," in *American Control Conference (ACC), 2014*, June 2014, pp. 4816–4823.
- [22] K. Moore, *Iterative Learning Control for Deterministic Systems*. London, UK: Springer-Verlag, 1993.
- [23] S. Mishra, U. Topcu, and M. Tomizuka, "Iterative learning control with saturation constraints," in *American Control Conference, 2009. ACC '09.*, June 2009, pp. 943–948.
- [24] F. Felici, "Real-Time Control of Tokamak Plasmas: from Control of Physics to Physics-Based Control," Ph.D. dissertation, Ecole Polytechnique Fédérale de Lausanne EPFL, Lausanne, 2011.
- [25] J. Nocedal and S. Wright, *Numerical Optimization*, 2nd ed., ser. Springer Series in Operations Research and Financial Engineering. Springer, 2006.
- [26] F. Hofmann, *et al.*, "Creation and control of variably shaped plasmas in TCV," *Plasma Physics and Controlled Fusion*, vol. 36, no. 12B, p. B277, 1994.
- [27] D. Humphreys, *et al.*, "Experimental vertical stability studies for ITER performance and design guidance," *Nuclear Fusion*, vol. 49, no. 11, p. 115003, 2009.
- [28] J.-M. Moret, *et al.*, "Tokamak equilibrium reconstruction code LIUQE and its real time implementation," *Fusion Engineering and Design*, vol. 91, no. 0, pp. 1 – 15, 2015.
- [29] A. Kallenbach, *et al.*, "Divertor power load feedback with nitrogen seeding in ASDEX Upgrade," *Plasma Physics and Controlled Fusion*, vol. 52, no. 5, p. 055002, 2010.
- [30] J. Bolder and T. Oomen, "Rational basis functions in iterative learning control - with experimental verification on a motion system," *IEEE Transactions on Control Systems Technology*, vol. 23, no. 2, pp. 722–729, 2015.